Design of Non-Destructive Evaluation Robot Using Magnetic Flux Leakage for Main Water Pipe

Jaekyu An
Manufacturing Robotics R&D Division
Korea Institute of Robot Convergence
Pohang, Republic of Korea
email: jkan@kiro.re.kr

Yong Sub Kwon
Manufacturing Robotics R&D Division
Korea Institute of Robot Convergence
Pohang, Republic of Korea
email: ys.kwon@kiro.re.kr

Soeun Son
Manufacturing Robotics R&D Division
Korea Institute of Robot Convergence
Pohang, Republic of Korea
email: smallsilver@kiro.re.kr

Eui-Jung Jung
Manufacturing Robotics R&D Division
Korea Institute of Robot Convergence
Pohang, Republic of Korea
email: ejjung@kiro.re.kr

Jongho Bae
Manufacturing Robotics R&D Division
Korea Institute of Robot Convergence
Pohang, Republic of Korea
email: jongho.bae@kiro.re.kr

Goobong Chung
Manufacturing Robotics R&D Division
Korea Institute of Robot Convergence
Pohang, Republic of Korea
email: goobongc@kiro.re.kr

***Abstract*—Many infrastructures in the world include pipe systems, e.g., gas, oil, water, electricity, air circulation, etc. Using a pipe system for the delivery of such materials allows for easy human control. However, if the pipe is broken or contaminated, the process is disturbed and the risk cost for the society can increase substantially. For instance, contaminations in fluids like air and water may result in spreading of diseases. Therefore, maintenance of the pipe is crucial. For a long period of time, identification of a pipe requiring a repair only depended on its installation time because its condition was not exposed until the pipe was destructed or cut. Recently, non-destructive evaluation technology and robotics are changing the paradigm of the identification process. Maintenance technicians can identify faulty pipes from reliable data, collected directly from the pipes, instead of relying on the pipe's installation period. In this paper, we propose a robot design with Non-Destructive Evaluation (NDE) for waterwork pipes.**

Keywords-main water pipe; waterworks; pipe; robot; NDE; MFL.

I. INTRODUCTION

A well-founded infrastructure plays a major role in city development. The infrastructure is composed of systems such as roads, electrical grids and water supply pipes. These systems are the power sources running the society. If one of the systems malfunctions, the society suffers from inconvenience and the productivity drops. Therefore, monitoring the conditions and maintenance of the infrastructure are directly correlated with the functionality of the society.

This paper discusses a design of NDE in-pipe robot for main water pipe. Many robots have already been used in water pipes [1] with various inspection technologies [2]. Among the various attributes of such robots, this research focuses on mobility using the Magnetic Flux Leakage (MFL) method [3].

The majority of existing NDE systems attempt to cover the whole pipe surface at the same time [4]. In order to cover the entire inner surface of the pipe, the system often requires a large number of attached sensors through the entire pipe. Our proposed design decreases the complexity by moving the sensors along the direction of the robot's movement. Also, to reduce the weight of the robot, our team considered a moving sensor as in the Diakont robot [7], which uses Electromagnetic Acoustic Transducer (EMAT). While this type of sensor increases the difficulty of the signal processing, our robot can still benefit in mobility by a reduction in the number of sensors. The robot can also smoothly carry the NDE modules at an inclined pipe, vertical pipe, elbow, and miter type pipe.

Additionally, there are two advantages using the MFL method. First, it is radiation free. Second, the method can be used to sense the magnetic field without the medium. These characteristics minimize possible water pollution that can occur during the pipe inspection.

Through this paper, we complete a complete design of the proposed robot. However, the future goal of the project is to make a system with MFL modules moving in spiral motion (Figure 1) when facing various obstacles. Consequently, the robot will be applied to real water main pipes. The results show the possibility of overcoming different obstacles present in pipes and a city will be able to have integrated control for maintenance of the pipes.

 ISBN: 978-1-61208-730-6

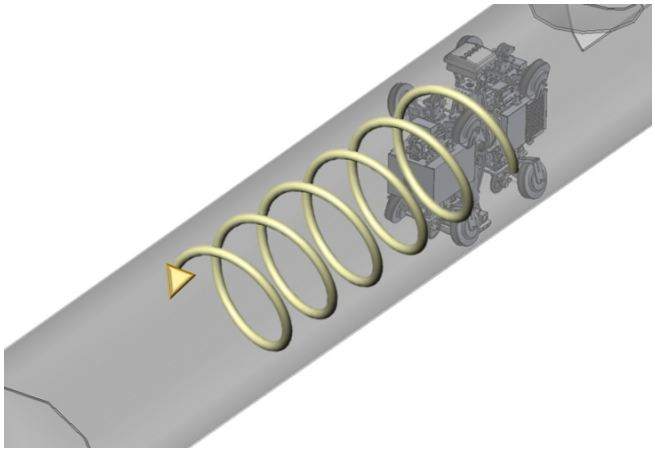

Figure 1. Example of the spiral motion of MFL modules.

II. DESIGN

A. System Overview

The targeted performances of the robot in this paper are stable spiral motion of the MFL modules and successful climbing of a 22.5° slope. We chose spiral motion because the spiral motion enables the robot to inspect the surface of the pipe with the minimum number of the MFL modules, resulting in a low system cost (weight, volume, power). The 22.5° slope is chosen because this is the value for the majority of water pipes in Republic of Korea.

To fulfill the set goals, the robot requires rotation, attachment and detachment actuators for the MFL module. A linkage system with sufficient wheel grip force is also required. Additionally, an odometer is required for locating the defects. Electrically, for the locomotion of the robot and visual inspection of the pipe condition, camera, Inertial Measurement Unit (IMU), Light Detection and Ranging (LiDAR), Single Board Computer (SBC), and Data acquisition (DAQ) for the MFL are installed as in Figure 2. Finally, the robot size is 1100 x 840~1100 x 300 (mm, L x H x W; height is changeable to adapt to the ovality of the pipe). The total weight is about 160 kg.

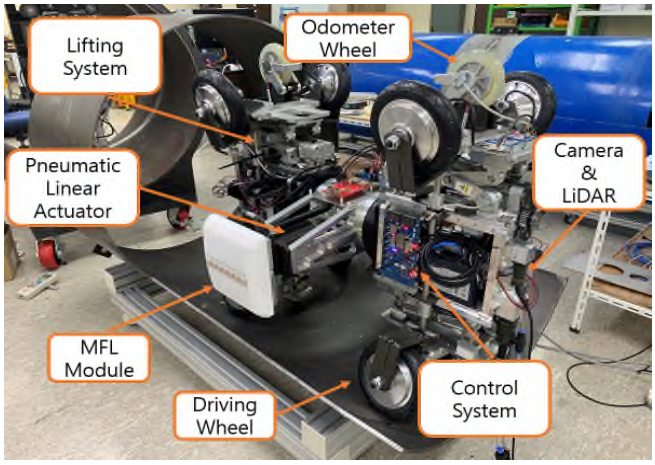

Figure 2. Components of the robot.

B. Free Body Diagram

Using free body diagram of the concept design and understanding about the system, the power of actuators effected by the attraction force of MFL and weight of the robot can be derived. MFL consists of magnet, hall sensor, front-back shoe, and Polytetrafluoroethylene (PTFE) cover, as shown in Figure 3. The hall sensor senses leakages of the magnetic field caused by reduction in pipe wall thickness. The PTFE cover is used to decrease the friction between the pipe and the MFL module.

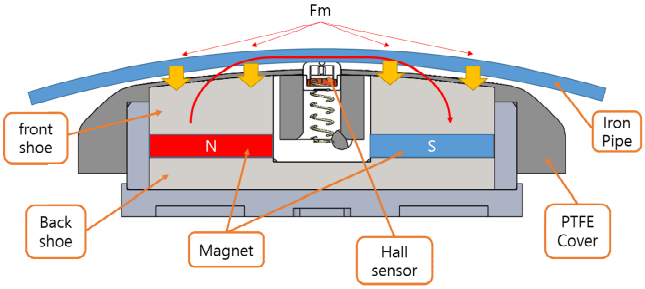

Figure 3. The MFL module section view: Shoes help to make closed magnetic field.

As depicted in Figure 4, the external forces are traction, drag force and weight. The traction force (F_{rt} : required traction force) is decided by the torque driving the wheel and the wheel grip force. The grip force is caused by the normal force on the wheel from the surface. The drag force of the MFL (F_{md}) is generated from the attraction force of magnet (F_m). The F_m can be calculated by (1). The size of the magnet is 150x56x10 (unit mm, L x W x H) and flux density is about 0.4 T (Tesla). The friction coefficient for PTFE and steel is about 0.2 [5]. Eventually, F_m and F_{md} are 2400 N and 480 N, respectively, because of two MFL modules. Additionally, on the slope, the weight of the robot creates a drag force. Therefore, considering the target acceleration motion, the required traction force can be obtained by (3), (4):

$$F_m = (B^2 \cdot A)/(2\mu_0) \quad (1)$$

B: flux density

μ_0 : the permeability of space($4\pi x10^{-7}$)

A: the area of each surface

$$F_{md} = \mu \cdot F_m \quad (2)$$

$$\Sigma F = ma = F_{rt} - F_{wx} - F_{md} \quad (3)$$

$$F_{rt} = ma + F_{wx} + F_{md} \quad (4)$$

The velocity and acceleration of the robot are 300 mm/s and 150 mm/s^2, respectively. The F_{rt} is about 1100 N. To generate the force, a torque of a wheel motor must be 33 Nm under the condition of eight wheels, 250 mm wheel diameter, and friction coefficient $\mu \cong 0.6$ between rubber (wheel tire) and steel [6]. For a stable locomotion, the non-slip condition of the wheel has to be considered. The condition states that the traction force generated by the

 ISBN: 978-1-61208-730-6

wheel torque should be smaller than the friction force of the tire (F_{nt}) created by the weight (refer to (5)). The current F_{nt} (680 N) is smaller than F_{rt} from (6). For a non-slip motion, F_{wy} can be increased by pushing on the pipe wall.

$$F_{nt} \geq F_{rt} \quad (5)$$

$$F_{nt} = \mu \cdot F_{wy} \quad (6)$$

Therefore, the minimum non-slip traction force is F_{rt}, which can be calculated from (7). Equations (8), (9) represent the traction force of the bottom and upper wheel, respectively.

$$Fnt = \mu \cdot (Fwy + F'p) + \mu \cdot Fp \quad (7)$$

$$Fbt = \mu \cdot (Fwy + F'p) \quad (8)$$

$$Fut = \mu \cdot Fp \quad (9)$$

$$Fp = F'p \quad (10)$$

$$Fp \geq (Frt - \mu \cdot Fwy) / (2 \cdot \mu) \quad (11)$$

By using F_p (380 N), upper (6 Nm) and bottom (27 Nm), the wheel torque is also calculated.

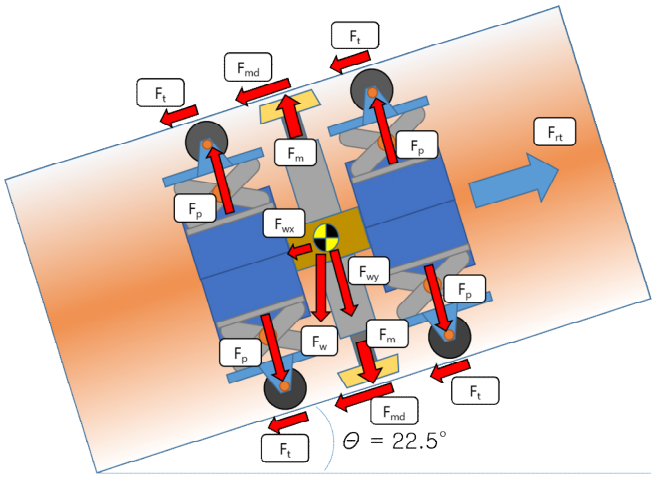

Figure 4. The free body diagram for understanding applied forces

C. Simulation for Driving Wheel Torque

To verify the result from the Free Body Diagram (FBD), we use a multibody dynamic analysis simulation tool: DAFUL [8]. Conditions used in DAFUL are equal to the values from the FBD, such as weight (1600 N), push force (380 N), drag force by MFL (480 N), and slope (22.5°), as in Figure 5. We are interested in the required torque in a wheel. Under these conditions, by substituting the target velocity of the wheel, DAFUL shows the resulting torque about the wheel. The average values for upper and bottom wheel are 20 Nm and 110 Nm, respectively. The robot system has eight wheels in total, 4 at the top and 4 at the bottom. Therefore, one top wheel needs about 5 Nm and one bottom wheel needs about 27 Nm, see Figure 6. The simulated values are shown to be very similar to our FBD results.

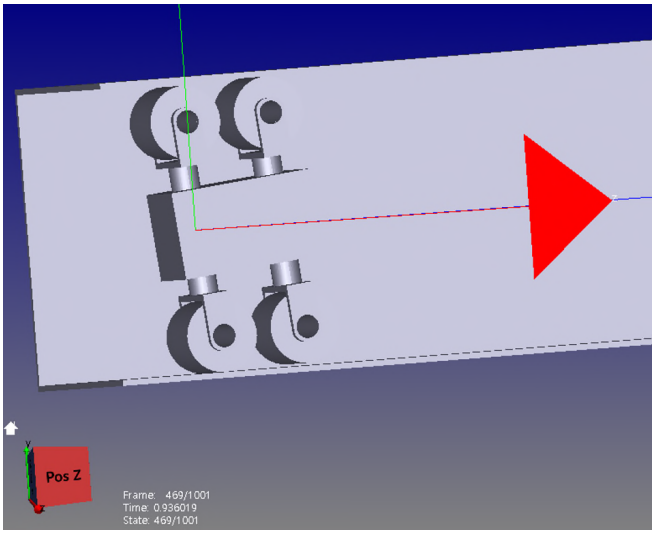

Figure 5. Simple modeling at the DAFUL

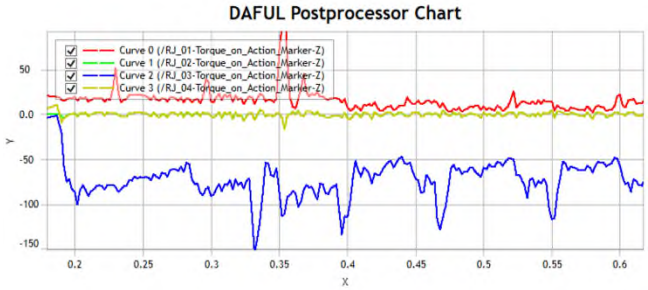

Figure 6. Results of Time (s) – Torque (Nm): the average of blue chart is about 27 Nm and red chart is about 5 Nm

D. MFL Rotation and Attachment Mechanism

MFL sensor modules have spiral motion with attaching condition on the pipe wall. It creates the friction force to be in a distracting rotational direction, as shown in the free body diagram section. The rotational torque can be found using equation (12):

$$\tau = d \times F_{md} \quad (12)$$

F_{md} from the two MFL modules is about 480 N and the torque is about 240 Nm. The pipe diameter is 1000 mm and the axis of rotation of the MFL is at the center of the pipe.

To sustain the torque and rotational velocity (30 rpm), a motor has to generate about 0.75 kW of power.

However, due to the large power source and motor volume, we try to generate detachment force (F_d) rather than turning to high power motors. The detachment force reduces the total MFL drag force from (13).

$$F_{md} = \mu \cdot (F_m - F_d) \quad (13)$$

 ISBN: 978-1-61208-730-6

To generate the F_d, pneumatic linear actuators are applied (Figure 7). Using calibrated pressure, the actuators are able to fully detach the MFL from the pipe wall or reduce the F_{md}.

The actuator is designed to generate a detachment force up to 1600 N at 0.65 MPa. By using the actuator, F_{md} decreased to 400 N resulting in a total required torque of 80 Nm and a motor power of 0.25 kW.

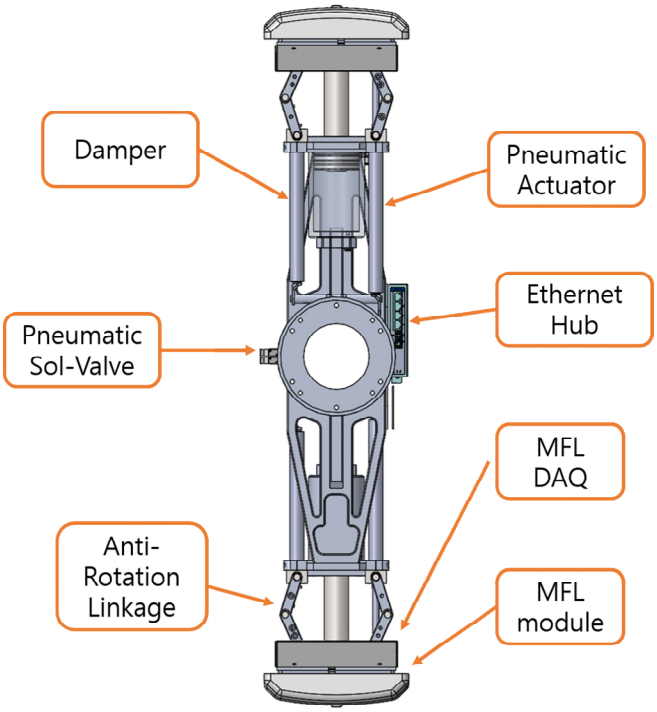

Figure 7. Rotating module: the MFL module and DAQ for sensing, Ethernet hub for transferring the sensing data to server, sol-valve for controlling the actuators, damper for reducing the sudden motion made by magnetic force

The MFL module can rotate infinitely which may twist the power and communication cables and air hose. To avoid the twist, a slip ring is applied and swivel manifold are specially designed. The swivel type causes the friction on the seal, which depends on the compressed volume of the O-ring. In our design, the volume is kept at half of the maximum recommended by the manufacturer, to decrease the friction, as in Figure 8.

Due to the decrease in the F_{md}, the required wheel torque is also decreased to 1 Nm (upper) and 22 Nm (bottom), allowing the choice of general hub motor.

E. Driving Wheel Attachment Mechanism

For a stable locomotion, wheels require a mechanism that creates a push force and conform to a rough pipe surface. A scissors mechanism is designed to lift the robot and push against the wall for stable attachment. The reaction force is the sum of push force and weight (14). The force is about 2000 N, weight 1600 N and push 380 N.

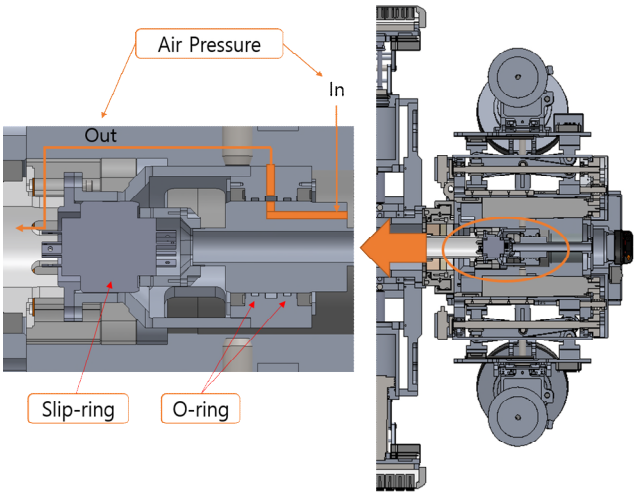

Figure 8. MFL modules rotating hinge mechanism

$$F_l = F_w + F_p \quad (14)$$

To generate the force, the mechanism (Figure 9) uses a ball screw which requires about 0.6 Nm of torque.

Because the ball screw cannot be driven backwards, the feedback current of the motor cannot be used to conform to the rough pipe surface and welding bead. In order to overcome this issue, we apply the load cell to directly read the external forces changed by pipe conditions.

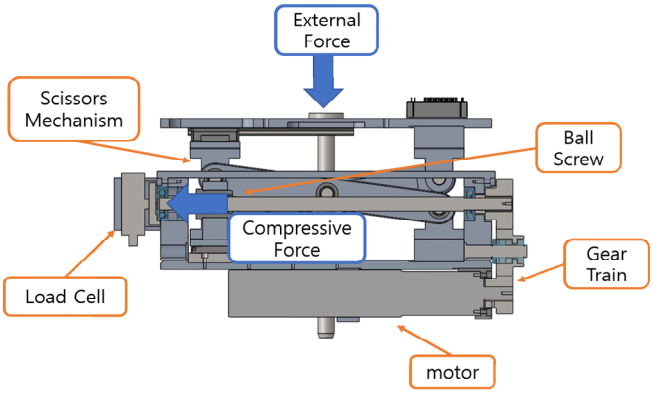

Figure 9. Wheel attachment mechanism

III. CONCLUSION

This project aims to design and verify robot mobility and motion of the sensors needed for a large water pipe inspection. As the result, we design a robot system that can climb a 22.5° slope and generate spiral motion for the sensors. The key design factor is the use of the pneumatic actuator. Using the compressibility of the air, compliance, control is made simple without additional force-torque

 ISBN: 978-1-61208-730-6

sensor, complex system modeling and control strategies compared to motor based systems. Additionally, because of reduced magnetic attractive force, the system's weight, volume and power consumption can be decreased with a low powered motor.

For the future work, we aim to overcome additional obstacles, such as 45° and 22.5° miter type bend, water, and spiral weld bead. Based on this research and development, we will design another robot system that will be able to overcome the additional obstacles marked in Figure 10. We will also develop an algorithm to find defects from data generated solely by the two MFL modules in spiral motion.

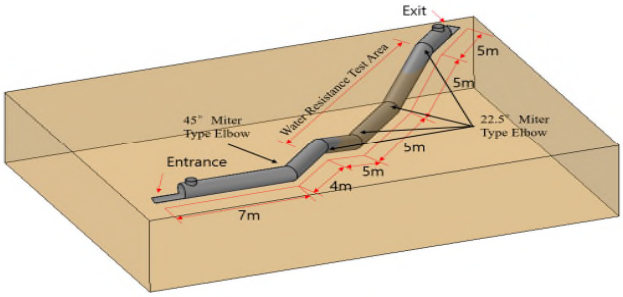

Figure 10. Final robot test bed: obstacles: 45°, 22.5° miter type elbow, water section, about 30 m distance.

ACKNOWLEDGMENT

This work was supported by Korea Environment Industry & Technology Institute (KEITI) through Advanced Water Management Research Program, funded by Korea Ministry of Environment (MOE) (RE201901020).

REFERENCES

[1] J. M. Mirats Tur and W. Garthwaite, "Robotic Devices for Water Main In-Pipe Inspection:A Survey," in J. Field Robotics, vol. 27, pp. 491-508, Apr. 2010, doi: 10.1002/rob.20347

[2] Z. Liu and Y. Kleiner, "State of the art review of inspection technologies for condition assessment of water pipes," in Measurement, vol. 46, pp. 1-15, Jan. 2013

[3] Y. Shi, C. Zhang, R. Li, M. Cai, and G. Jia, "Theory and Application of Magnetic Flux Leakage Pipeline Detection," in Sensors, vol. 15(12), pp. 31036-31055, Dec., 2015

[4] H. Song, L. Yang, G. Liu, G. Tian, D. Ona, Y. Song, and S. Li," Comparative Analysis of In-line Inspection Equipments and Technologies," in IOP Conf. Ser.: Mate. Sci. Eng., vol. 382, pp. 032021, Jul. 2018

[5] W. G. Sawyer, K. D. Freudenberg, P. Bhimaraj, and L. S. Schadler, "A study on the friction and wear behavior of PTFE filled with alumina nanoparticles," in Wear, vol. 254, pp 573-580, Mar. 2003.

[6] M. A. Cruz Gómez, E. A. Gallardo-Hernández, M. Vite Torres, and A. Peña Bautista, "Rubber steel friction in contaminated contacts," in Wear, vol. 302, pp. 1421-1425, Feb. 2013.

[7] Diakont, http://www.diakont.com/energy_services/robotic_inline_inspection.html [accessed July 2019]

[8] C. W. Rim, J. S. Bang, S. J. Moon, T. Y. Chung, H. J. Cho, and D. S. Bae, "Development of Software for Coupled Aero-Elastic Dynamic Analysis of Wind Turbine System," in International Society of Offshore and Polar Engineers, Jan. 2010.

 ISBN: 978-1-61208-730-6